

A machine learning-based dependence coefficient for gene expression analysis

This manuscript ([permalink](#)) was automatically generated from [greenelab/clustermatch-gene-expr-manuscript@abe8f12](#) on January 5, 2022.

Draft

This manuscript version is work-in-progress

Authors

- **Milton Pivdori**

 [0000-0002-3035-4403](#) ·  [miltondp](#) ·  [miltondp](#)

Department of Genetics, Perelman School of Medicine, University of Pennsylvania, Philadelphia, PA 19104, USA ·

Funded by The Gordon and Betty Moore Foundation GBMF 4552; The National Human Genome Research Institute (R01 HG010067)

- **Marylyn D. Ritchie**

 [0000-0002-1208-1720](#) ·  [MarylynRitchie](#)

Department of Genetics, Perelman School of Medicine, University of Pennsylvania, Philadelphia, PA 19104, USA

- **Diego H. Milone**

 [0000-0003-2182-4351](#) ·  [dmilone](#) ·  [d1001](#)

Research Institute for Signals, Systems and Computational Intelligence (sinc(i)), Universidad Nacional del Litoral, Consejo Nacional de Investigaciones Científicas y Técnicas (CONICET), Santa Fe CP3000, Argentina

- **Casey S. Greene**

 [0000-0001-8713-9213](#) ·  [cgreene](#) ·  [GreeneScientist](#)

Center for Health AI, University of Colorado School of Medicine, Aurora, CO 80045, USA; Department of Biochemistry and Molecular Genetics, University of Colorado School of Medicine, Aurora, CO 80045, USA · Funded by The Gordon and Betty Moore Foundation (GBMF 4552); The National Human Genome Research Institute (R01 HG010067); The National Cancer Institute (R01 CA237170)

Abstract

Introduction

Results

A robust and efficient not-only-linear dependence coefficient

Clustermatch is a dependence coefficient that can compute a similarity measure between any pair of variables, either with numerical or categorical values [1]. The method assumes that if there is a relationship between two variables/features describing n data points/objects, then the clusterings on those n objects derived using each variable individually should match (see Methods). Although different clustering algorithms can be applied to one-dimensional data [2], we used quantiles to efficiently separate data points into different clusters (i.e., the median separates numerical data into two clusters). Since in Clustermatch the data is categorized into clusters, numerical and categorical data can be naturally integrated since clusters do not need an order. Once all internal partitions from each variable are generated, the Clustermatch coefficient is defined as the maximum adjusted Rand index (ARI) [3] between them. We previously compared Clustermatch [1] with the Maximal Information Coefficient (MIC) [4] and Distance Correlation (DC) [5], two popular nonlinear correlation coefficients. In addition to outperforming these two methods in a simulated scenario with different noise levels, Clustermatch was also significantly superior on computational complexity, making it the only practical not-only-linear coefficient for real and large datasets such as gene expression compendia. Therefore, in this study we will only focus on Clustermatch and two widely used ones: Pearson and Spearman.

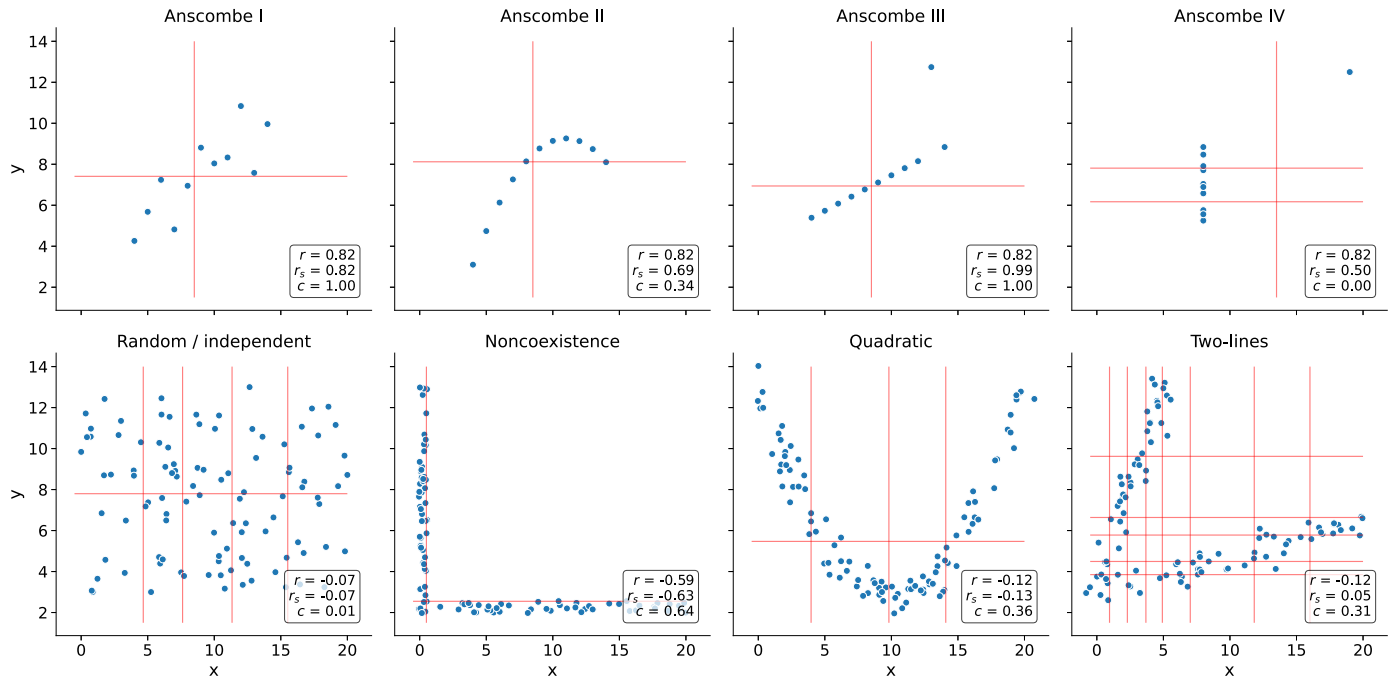


Figure 1: Different types of relationships in data. Each panel contains a set of simulated data points described by two variables: x and y . The first row shows the Anscombe's quartet with four different datasets (from Anscombe I to IV) with 11 data points each. The second row contains another set of general patterns with 100 data points each. Each panel shows the correlation value using the Pearson (r), Spearman (r_s) and Clustermatch (c) coefficients. Vertical and horizontal lines show how Clustermatch separated data points using x and y , respectively.

In Figure 1, we show how Pearson (r), Spearman (r_s) and Clustermatch (c) behave on different data patterns, where red lines indicate how Clustermatch clusters data points using each feature

individually (either x or y). In the first row of the figure, the Anscombe's quartet [6] is shown, which comprises four synthetic datasets with completely different patterns but exactly the same data statistics (mean, standard deviation and Pearson's correlation). This kind of simulated data, including also the "Datasaurus" [7,8,9], are frequently used as a reminder of the importance of going beyond simple statistics, where either undesirable patterns (such as outliers) or desirable ones (such as non-linear relationships reflecting real and complex biological relationships) can be masked by these numbers. For example, Anscombe I seems to show a noisy but clear linear pattern, similar to Anscombe III where the linearity is perfect besides one outlier. For these two patterns, Clustermatch separates these data points using two clusters (one red line for each variable x and y), yielding 1.0, the maximum value, correctly identifying the relationship. Anscombe II seems to follow a quadratic distribution, and this is reflected in the Clustermatch with a lower yet non-zero value of 0.34. Anscombe IV shows a vertical line where x values are almost constant except for one outlier. This outlier does not influence Clustermatch as it does for Pearson or Spearman, and thus $c = 0.00$ (the minimum value) indicates no association for this variable pair because it does not fit the Clustermatch assumption: the two clusters formed with x (approximately separated by $x = 13$) do not match well the three clusters formed with y . The Pearson's correlation coefficient is the same across all these Anscombe's examples ($r = 0.82$) whereas Spearman is always above or equal to 0.50. The reason for this behavior is that these coefficients are based on data statistics such as the mean, standard deviation and, in the case of Spearman, data rankings, and this falls short in dealing with noisy data.

The second row of Figure 1 shows other simulated relationships with general nonlinear patterns, some of which were previously observed in gene expression data [4,10,11]. For the random/independent pair of variables, all coefficients correctly agree with a value close to zero. In this case, Clustermatch separates data points into five clusters using x and two using y , which do not match thus yielding $c = 0.01$. For the other three examples (quadratic, noncoexistence and two-lines), Pearson and Spearman generally fail to capture a clear pattern between variables x and y . These patterns also show how Clustermatch uses different degrees of complexity to capture the relationships. For the noncoexistence pattern, where for instance one gene (x) might be expressed while the other one (y) is inhibited, Clustermatch only needs two clusters for both variables, similarly to a linear relationship (Anscombe I and III). For the quadratic pattern, Clustermatch separates x into more clusters (four in this case) to reach the maximum ARI. The two-lines example shows two embedded linear relationships, not detected by either Pearson or Spearman, and for which Clustermatch separates in eight clusters for x and six for y .

Datasets such as Anscombe or "Datasaurus" highlight the need of visualization before drawing conclusions on summary statistics alone. Although extra steps such as visual analyses are always mandatory, larger datasets make it impossible to perform manual assessment on each, for example, gene pair. More advanced techniques, such as Clustermatch, could reduce the number of false positives/negatives to focus human validation on patterns that are more likely to be real. Clustermatch has only one parameter: k_{\max} , which is 10 by default, is the maximum number of internal clusters that the algorithm will use when partitioning data points using each variable. As we showed in the examples above, this parameter can control the level of complexity the end-user desires to capture. A value of $k_{\max} = 2$ makes the coefficient more leaned towards linear patterns, whereas higher values can detect other, more complex kinds of relationships. We found that $k_{\max} = 10$ approximates well the coefficient values for different types of patterns [1] while balancing computing time and keeping a close-to-zero value for random data, which is guaranteed by the adjusted-for-chance property of ARI [12].

In the next sections we compare there coefficients on real gene expression data and highlight some complex and potentially interesting relationships.

Clustermatch detects linear and nonlinear patterns in human transcriptomic data

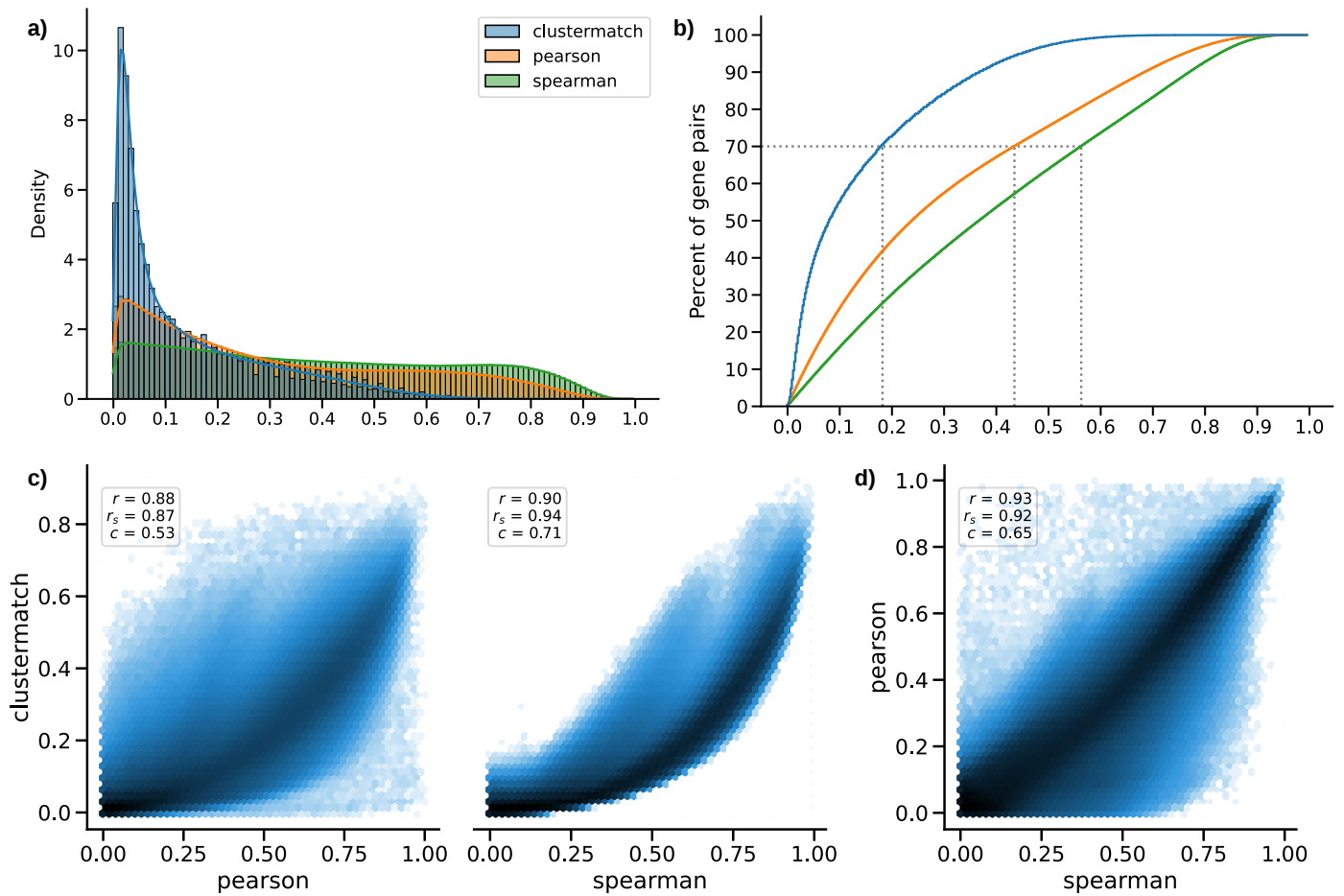


Figure 2: Distribution of coefficient values on gene expression (GTEx v8, whole blood). **a)** Histogram of coefficient values. **b)** Corresponding cumulative histogram. The dotted line maps the coefficient value that accumulates 70% of gene pairs. **c)/d)** 2D histogram plot with hexagonal bins between all coefficients, where a logarithmic scale was used to color each hexagon.

We used gene expression data from GTEx v8 and selected the top five tissues with more sample size: muscle (skeletal), whole blood, skin (sun exposed), adipose (subcutaneous) and artery (tibial). For each of these tissues, we selected the top 5,000 genes with largest variance, and then computed the pairwise correlation matrix using Pearson, Spearman and Clustermatch. In Figure 2 a, we show how the pairwise correlation values distribute in whole blood, where Clustermatch (mean=0.14, median=0.08, sd=0.15) has a much more skewed distribution than Pearson (mean=0.31, median=0.24, sd=0.24) and especially Spearman (mean=0.39, median=0.37, sd=0.26). Each coefficient reaches 70% of gene pairs at $c = 0.18$, $r = 0.44$ and $r_s = 0.56$ (Figure 2 b, respectively). When we directly compare each coefficient with each other, the agreement between Clustermatch and Spearman is higher than any of these with Pearson (Figures 2 c and d).

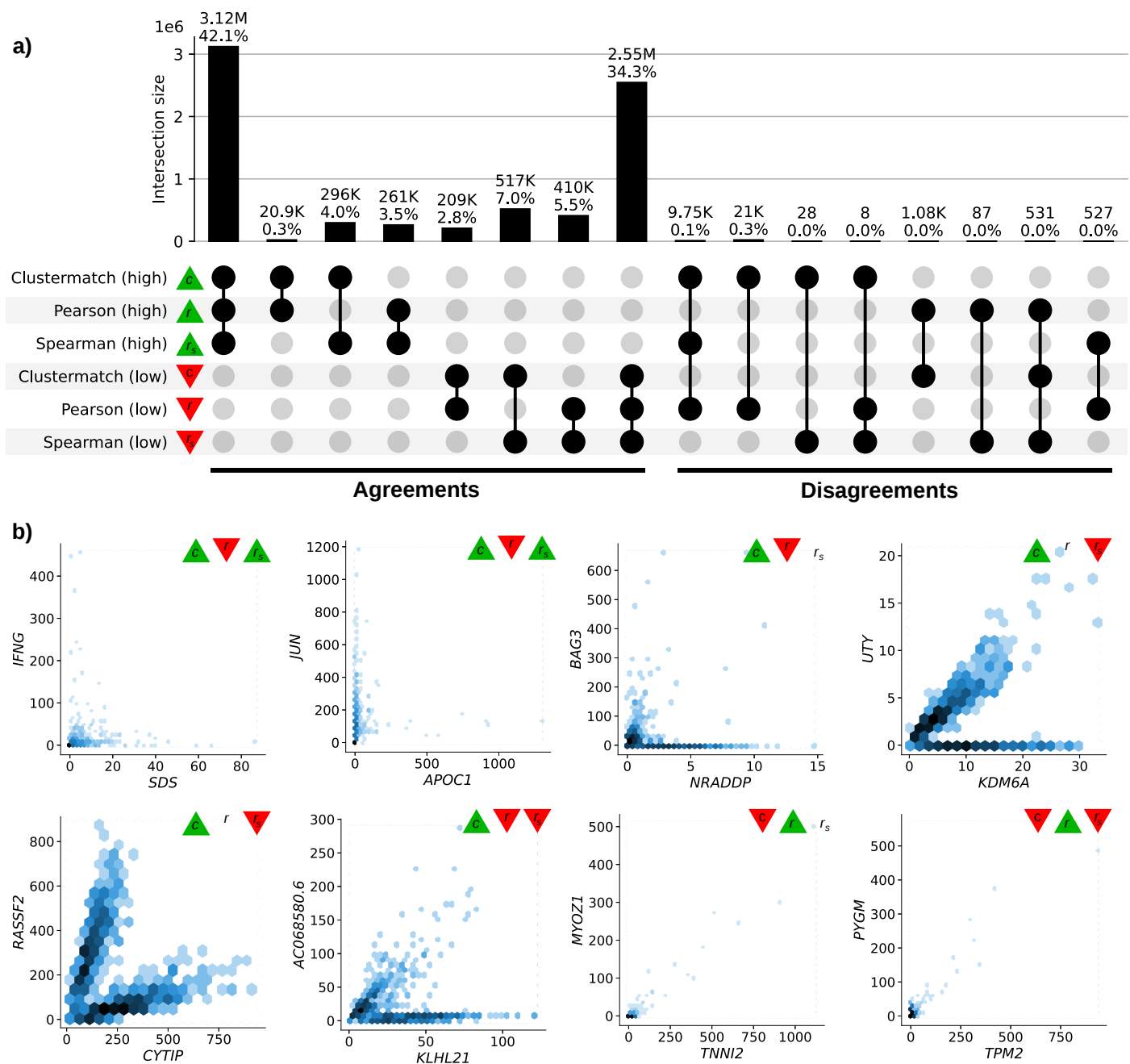


Figure 3: Intersection of gene pairs with high and low coefficient values (GTEx v8, whole blood). **a)** UpSet plot with six categories (rows) with the highest and lowest 30% correlation values. Columns show different intersections of categories grouped by agreements and disagreements. **b)** Hexagonal binning plots with examples of gene pairs where Clustermatch (c) disagrees with Pearson (r) and Spearman (r_s). A logarithmic scale was used to color each hexagon.

A closer inspection of gene pairs detected and missed by these coefficients revealed the ability of Clustermatch to capture more complex yet biologically meaningful patterns. For this, we analyzed the agreements and disagreements by obtaining for each coefficient the top 30% of gene pairs with the largest correlation values (a “high” set) and the bottom 30% (“low”), resulting in six potentially overlapping categories. An UpSet plot [13] is shown in Figure 3 a, where the intersections of these six categories allowed to precisely identify the gene expression patterns captured and missed by each coefficient. The three coefficients agree more on gene pairs with a high correlation value (42.1%) than on those with no relationship (34.3%). The figure also confirms that Clustermatch and Spearman agree more on highly correlated pairs (4.0% in “high”, and 7.0% in “low”) than any of these with Pearson (all between 0.3%-3.5% for “high”, and 2.8%-5.5% for “low”). Regarding disagreements, there are thousands of gene pairs with a high Clustermatch value that are not detected by the other coefficients. There are also gene pairs with a high Pearson value that have either low Clustermatch (1,075) or low Clustermatch and low Spearman values (531). However, these cases mostly seem to be driven by outliers (Figure 3 b). No gene pairs highly ranked by Spearman are missed by Clustermatch.

In Figure 3 b, we show individual examples of gene pairs where Clustermatch disagrees with Pearson, Spearman or both. Genes *UTY* (chromosome Y) and *KDM6A* (chromosome X), which are paralogs, show a nonlinear relationship with a subset of samples (males) following a strong linear pattern, and another subset (females) having a constant expression of one gene (*UTY* is zero in this case, as expected). This combination of linear and constant patterns is captured by Clustermatch ($c = 0.29$) but not by Pearson and Spearman ($r = 0.24, r_s = 0.10$). Clustermatch also correctly identifies this gene pair pattern in all other tissues in GTEx with the exception of female-specific organs (Supplementary Figures 5). Another composite relationship is present for genes *RASSF2* (20p13) and *CYTIP* (2q24.1) which show two clear linear patterns. These two genes are strongly expressed in white blood cells, both in myeloid and lymphoid lineages, and using tissue-specific gene networks from GIANT [14] we found strong evidence of interactions in these cell types (Supplementary Figure 4).

Discussion

Methods

Clustermatch algorithm

Algorithm 1: Clustermatch algorithm

```

1 Function get_partitions( $\mathbf{v}, k_{\max}$ ):
    Output:
         $\Omega_r$ : clustering with  $r$  clusters over  $n$  objects
2 if  $\mathbf{v} \in \mathbb{R}^n$  then
3     for  $r \leftarrow 2$  to  $\min\{k_{\max}, |\mathbf{v}| - 1\}$  do
4          $\rho \leftarrow (\rho_\ell \mid \Pr(v_i < \rho_\ell) \leq (\ell - 1)/r), \forall \ell \in [1, r + 1]$ 
5          $\Omega_{r\ell} \leftarrow \{i \mid \rho_\ell < v_i \leq \rho_{\ell+1}\}, \forall \ell \in [1, r]$ 
6     else
7         // TODO: not implemented yet in optimized version
8          $\mathcal{C} \leftarrow \cup_j \{v_i\}$ 
9          $r \leftarrow |\mathcal{C}|$ 
10         $\Omega_{rc} \leftarrow \{i \mid v_i = \mathcal{C}_c\}, \forall c \in [1, r]$ 
11        // TODO: remove singletons
12    return  $\Omega$ 
13
14 Function clustermatch( $\mathbf{x}, \mathbf{y}, k_{\max}$ ):
    Input:
         $\mathbf{x}$ : feature values on  $n$  objects
         $\mathbf{y}$ : feature values on  $n$  objects
         $k_{\max}$ : maximum number of internal clusters
    Output:
         $c$ : similarity value for  $\mathbf{x}$  and  $\mathbf{y}$  ( $c \in [0, 1]$ )
15  $\Omega^{\mathbf{x}} = \text{get\_partitions}(\mathbf{x}, k_{\max})$ 
16  $\Omega^{\mathbf{y}} = \text{get\_partitions}(\mathbf{y}, k_{\max})$ 
17  $c \leftarrow \max\{\mathcal{A}(\Omega_p^{\mathbf{x}}, \Omega_q^{\mathbf{y}})\}, \forall p, q$ 
18 return  $c$ 

```

References

1. **Clustermatch: discovering hidden relations in highly diverse kinds of qualitative and quantitative data without standardization**
Milton Pividori, Andres Cernadas, Luis A de Haro, Fernando Carrari, Georgina Stegmayer, Diego H Milone
Bioinformatics (2019-06-01) <https://doi.org/gfg4bt>
DOI: [10.1093/bioinformatics/bty899](https://doi.org/10.1093/bioinformatics/bty899) · PMID: [30357313](https://pubmed.ncbi.nlm.nih.gov/30357313/)
2. **The Data Model Concept in Statistical mapping**
George F Jenks
International Yearbook of Cartography (1967)
3. **Comparing partitions**
Lawrence Hubert, Phipps Arabie
Journal of Classification (1985-12) <https://doi.org/bpnmzh>
DOI: [10.1007/bf01908075](https://doi.org/10.1007/bf01908075)
4. **Detecting Novel Associations in Large Data Sets**
David N Reshef, Yakir A Reshef, Hilary K Finucane, Sharon R Grossman, Gilean McVean, Peter J Turnbaugh, Eric S Lander, Michael Mitzenmacher, Pardis C Sabeti
Science (2011-12-16) <https://doi.org/bzn5c3>
DOI: [10.1126/science.1205438](https://doi.org/10.1126/science.1205438) · PMID: [22174245](https://pubmed.ncbi.nlm.nih.gov/22174245/) · PMCID: [PMC3325791](https://pubmed.ncbi.nlm.nih.gov/PMC3325791/)
5. **Measuring and testing dependence by correlation of distances**
Gábor J Székely, Maria L Rizzo, Nail K Bakirov
The Annals of Statistics (2007-12-01) <https://doi.org/dkgjb4>
DOI: [10.1214/009053607000000505](https://doi.org/10.1214/009053607000000505)
6. **Graphs in Statistical Analysis**
FJ Anscombe
The American Statistician (1973-02) <https://doi.org/gfpm48>
DOI: [10.1080/00031305.1973.10478966](https://doi.org/10.1080/00031305.1973.10478966)
7. **Download the Datasaurus: Never trust summary statistics alone; always visualize your data**
Alberto Cairo
<http://www.thefunctionalart.com/2016/08/download-datasaurus-never-trust-summary.html>
8. **Same Stats, Different Graphs: Generating Datasets with Varied Appearance and Identical Statistics through Simulated Annealing**
Justin Matejka, George Fitzmaurice
Proceedings of the 2017 CHI Conference on Human Factors in Computing Systems (2017-05-02) <https://doi.org/gdtg2w>
DOI: [10.1145/3025453.3025912](https://doi.org/10.1145/3025453.3025912) · ISBN: 9781450346559
9. **Generating data sets for teaching the importance of regression analysis**
Lori L Murray, John G Wilson
Decision Sciences Journal of Innovative Education (2021-04) <https://doi.org/gjmggt>
DOI: [10.1111/dsji.12233](https://doi.org/10.1111/dsji.12233)
10. **A Novel Method to Efficiently Highlight Nonlinearly Expressed Genes**
Qifei Wang, Haojian Zhang, Yuqing Liang, Heling Jiang, Siqiao Tan, Feng Luo, Zheming Yuan, Yuan Chen

Frontiers in Genetics (2020-01-31) <https://doi.org/gnr5k7>
DOI: [10.3389/fgene.2019.01410](https://doi.org/10.3389/fgene.2019.01410) · PMID: [32082366](https://pubmed.ncbi.nlm.nih.gov/32082366/) · PMCID: [PMC7006292](https://pubmed.ncbi.nlm.nih.gov/PMC7006292/)

11. **Comprehensive Identification of Cell Cycle-regulated Genes of the Yeast *Saccharomyces cerevisiae* by Microarray Hybridization**
Paul T Spellman, Gavin Sherlock, Michael Q Zhang, Vishwanath R Iyer, Kirk Anders, Michael B Eisen, Patrick O Brown, David Botstein, Bruce Futcher
Molecular Biology of the Cell (1998-12) <https://doi.org/gnr5k5>
DOI: [10.1091/mbc.9.12.3273](https://doi.org/10.1091/mbc.9.12.3273) · PMID: [9843569](https://pubmed.ncbi.nlm.nih.gov/9843569/) · PMCID: [PMC25624](https://pubmed.ncbi.nlm.nih.gov/PMC25624/)
12. **Information Theoretic Measures for Clusterings Comparison: Variants, Properties, Normalization and Correction for Chance**
Nguyen Xuan Vinh, Julien Epps, James Bailey
Journal of Machine Learning Research (2010) <http://www.jmlr.org/papers/v11/vinh10a.html>
13. **UpSet: Visualization of Intersecting Sets**
Alexander Lex, Nils Gehlenborg, Hendrik Strobelt, Romain Vuillemot, Hanspeter Pfister
IEEE Transactions on Visualization and Computer Graphics (2014-12-31) <https://doi.org/f3ssr5>
DOI: [10.1109/tvcg.2014.2346248](https://doi.org/10.1109/tvcg.2014.2346248) · PMID: [26356912](https://pubmed.ncbi.nlm.nih.gov/26356912/) · PMCID: [PMC4720993](https://pubmed.ncbi.nlm.nih.gov/PMC4720993/)
14. **Understanding multicellular function and disease with human tissue-specific networks**
Casey S Greene, Arjun Krishnan, Aaron K Wong, Emanuela Ricciotti, Rene A Zelaya, Daniel S Himmelstein, Ran Zhang, Boris M Hartmann, Elena Zaslavsky, Stuart C Sealfon, ... Olga G Troyanskaya
Nature genetics (2015-06) <https://www.ncbi.nlm.nih.gov/pmc/articles/PMC4828725/>
DOI: [10.1038/ng.3259](https://doi.org/10.1038/ng.3259) · PMID: [25915600](https://pubmed.ncbi.nlm.nih.gov/25915600/) · PMCID: [PMC4828725](https://pubmed.ncbi.nlm.nih.gov/PMC4828725/)
15. **RASSF2, CYTIP - HumanBase** <https://hb.flatironinstitute.org/gene/9770+9595>

Acknowledgements

Supplementary material

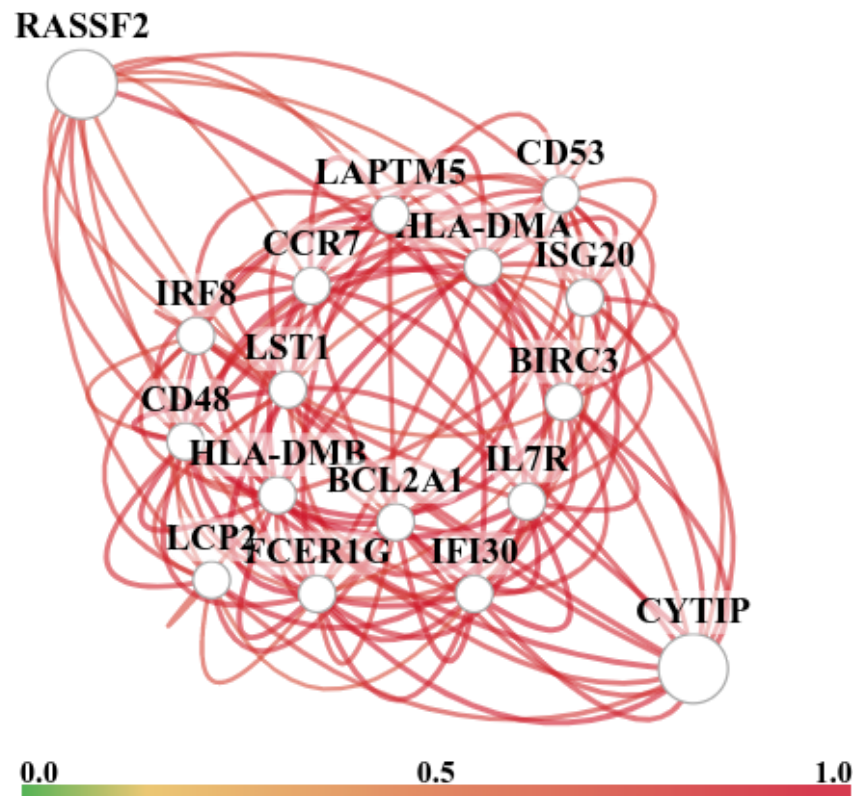


Figure 4: Predicted interactions between *RASSF2* and *CYTIP* in white blood cells (leukocytes). Nodes represent genes and edges are the probability that the gene pair is part of the same biological process in leukocytes. This analysis can be performed online using HumanBase [\[15\]](#).

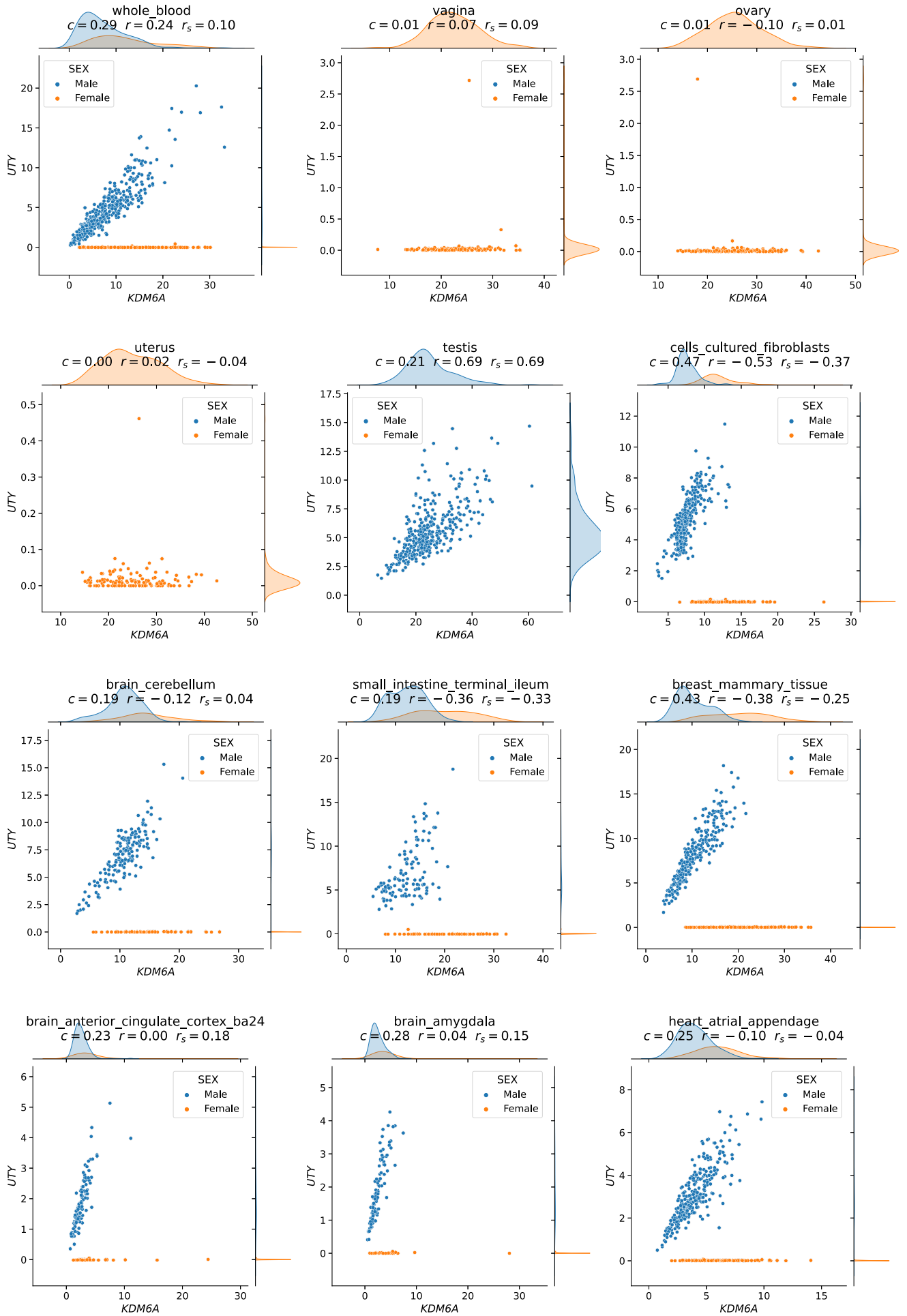


Figure 5: Scatter plots of genes *KDM6A* and *UTY* across different GTEx tissues.